

# Simulation of beam-beam effects and Tevatron experience

---

**Alexander Valishev<sup>a\*</sup>, Yuri Alexahin<sup>a</sup>, Valeri Lebedev<sup>a</sup> and Dmitry Shatilov<sup>b</sup>**

*<sup>a</sup>Fermi National Accelerator Laboratory,  
PO Box 500, Batavia, IL, 60510 USA*

*<sup>b</sup>Budker Institute of Nuclear Physics,  
Novosibirsk, 630090, Russia  
E-mail: valishev@fnal.gov*

**ABSTRACT:** Effects of electromagnetic interactions of colliding bunches in the Tevatron had a variety of manifestations in beam dynamics presenting vast opportunities for development of simulation models and tools. In this paper the computer code for simulation of weak-strong beam-beam effects in hadron colliders is described. We report the collider operational experience relevant to beam-beam interactions, explain major effects limiting the collider performance and compare results of observations and measurements with simulations.

**KEYWORDS:** Beam-beam; Collider; Beam dynamics.

---

\*Corresponding author.

---

## Contents

<b>1. Introduction</b>	<b>1</b>
<b>2. Overview of beam-beam effects</b>	<b>2</b>
2.1 Beam-beam effects at injection	3
2.2 Low-beta squeeze	3
2.3 High energy physics	4
<b>3. Store beam physics analysis</b>	<b>7</b>
<b>4. Weak-strong code Lifetrac</b>	<b>8</b>
4.1 Tevatron optics	9
4.2 Chromaticity	10
4.3 Diffusion and noise	10
4.4 Program features	13
4.5 Code validation	13
<b>5. Simulation results</b>	<b>14</b>
5.1 Optics errors	14
5.2 New collision helix	15
5.3 Chromaticity	16
5.4 $\beta^*$ reduction	17
5.5 Second order chromaticity	17
<b>6. Summary and discussion</b>	<b>19</b>

---

## 1. Introduction

Peak luminosity of the Tevatron reached  $4.3 \times 10^{32} \text{ cm}^{-2}\text{s}^{-1}$ , which exceeds the original Run II goal [1]. This achievement became possible due to numerous upgrades in the antiproton source, injector chain, and in the Tevatron collider itself. The most notable rise of luminosity came from the commissioning of electron cooling in the recycler ring and advances in the antiproton accumulation rate [2]. Starting from 2007, the intensity and brightness of antiprotons delivered to the collider greatly enhanced the importance of beam-beam effects. Several configurational and operational improvements in the Tevatron have been planned and implemented in order to alleviate these effects and allow stable running at high peak luminosities.

Since the publication of paper [3] that gave a detailed summary of beam dynamics issues related to beam-beam effects, the peak luminosity of Tevatron experienced almost a tree-fold increase. In the present article we provide an updated view based on the last years of collider operation (Section 2).

Development of a comprehensive computer simulation of beam-beam effects in the Tevatron started in 1999. This simulation proved to be a useful tool for understanding existing limitations and finding ways to mitigate them. In Section 4 the main features of the code Lifetrac are described. In Sections 5.2-5.5 we summarize our experience with simulations of beam-beam effects in the Tevatron, and cross-check the simulation results against various experimental data and analytical models. We also correlate the most notable changes in the machine performance to changes of configuration and beam conditions, and support the explanations with simulations.

## 2. Overview of beam-beam effects

A detailed description of the Tevatron collider Run II is available in other sources [1]. Here only the essential features important for understanding of beam dynamics are provided.

The Tevatron was a superconducting proton-antiproton collider ring in which beams of the two species collided at the center of mass energy of  $2 \times 0.98$  TeV at two experiments. Each beam consisted of 36 bunches grouped in 3 trains of 12 with 396 ns bunch spacing and  $2.6 \mu\text{s}$  abort gaps between the trains. The beams shared a common vacuum chamber with both beams moving along helical trajectories formed by electrostatic separators. Before the high energy physics collisions have been initiated, the proton and antiproton beams could be moved longitudinally with respect to each other, which is referred to as cogging. This configuration allowed for 72 interactions per bunch each turn with the total number of collision points in the ring equal to 138. The total number of collision points was determined by the symmetry of bunch filling pattern.

At the peak performance Tevatron operated with approx.  $N_p = 2.8 \cdot 10^{11}$  protons and  $N_a = 0.9 \cdot 10^{11}$  antiprotons per bunch at the beginning of a store. The normalized transverse 95% beam emittances were  $\varepsilon_p = 18 \cdot 10^{-6}\text{m}$  for protons and  $\varepsilon_a = 7 \cdot 10^{-6}\text{m}$  for antiprotons. Proton and antiproton bunch length at the beginning of a high energy physics (HEP) store was 52 cm and 48 cm, respectively. Parameters of the beams were mostly determined by the upstream machines.

The value of  $\beta$ -function at the main collision points ( $\beta^*$ ) was 0.28 m. Betatron tunes were  $Q_x = 20.584$ ,  $Q_y = 20.587$  for protons and  $Q_x = 20.575$ ,  $Q_y = 20.569$  for antiprotons.

A typical collider fill cycle is shown in Fig. 1. First, proton bunches were injected one at a time on the central orbit. After that, the electrostatic separators were powered and antiproton bunches were injected in batches of four. This process was accompanied by longitudinal cogging after each 3 transfers. Then the beams were accelerated to the top energy (85 s) and the machine optics was changed to collision configuration in 25 steps over 120 seconds (low-beta squeeze). The last two stages included initiating collisions at the two main interaction points (IP) and removing halo by moving in the collimators.

It has been shown in machine studies that beam losses up the ramp and through the low-beta squeeze were mainly caused by beam-beam effects [3]. In the HEP mode, the beam-beam induced emittance growth and particle losses contributed to the faster luminosity decay. Figure 2 summarizes the observed losses of luminosity during different stages of the collider cycle.

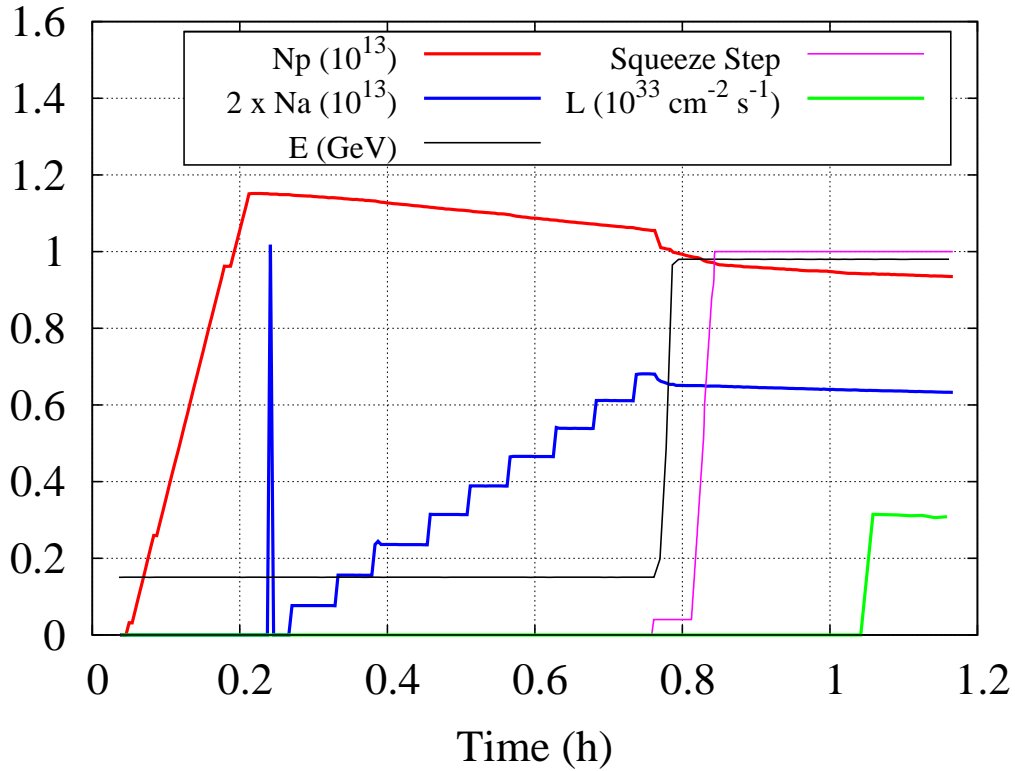


**Figure 1.** Collider fill cycle for store 5989.

## 2.1 Beam-beam effects at injection

During injection the long range (also referred to as parasitic) beam-beam effects caused proton losses (usually 5 to 10%). At the same time the antiproton life time was very good and only a fraction of a per cent were lost. Observations showed that mainly off momentum particles were lost (Fig. 3) and the betatron tune chromaticity  $C = dQ/d\delta$ , where  $\delta = \Delta p/p$  is the relative momentum deviation, had a remarkable effect. Early in Run II the chromaticity had to be kept higher than 8 units in order to maintain coherent stability of the intense proton beam, but after several improvements aimed at reduction of the machine impedance the chromaticity was about 3 units [4, 5, 6]. Figure 3 shows an interesting feature in the behavior of two adjacent proton bunches (no. 20 and 21). Spikes in the measured values are instrumental effects labeling the time when the beams are clogged. Before the first clogging the bunches have approximately equal life time. After the first clogging bunch 20 exhibits faster decay, and bunch 21 after the second. Analysis of the collision patterns for these bunches allowed to pinpoint a particular collision point responsible for the life time degradation. The new injection helix has been implemented late in 2007 which improved the proton life time [7, 8].

## 2.2 Low-beta squeeze

During the low-beta squeeze two significant changes occurred - the  $\beta^*$  value was being gradually decreased from  $\sim 1.5$  m to 0.28 m (hence the name squeeze) and the helical orbits changed their

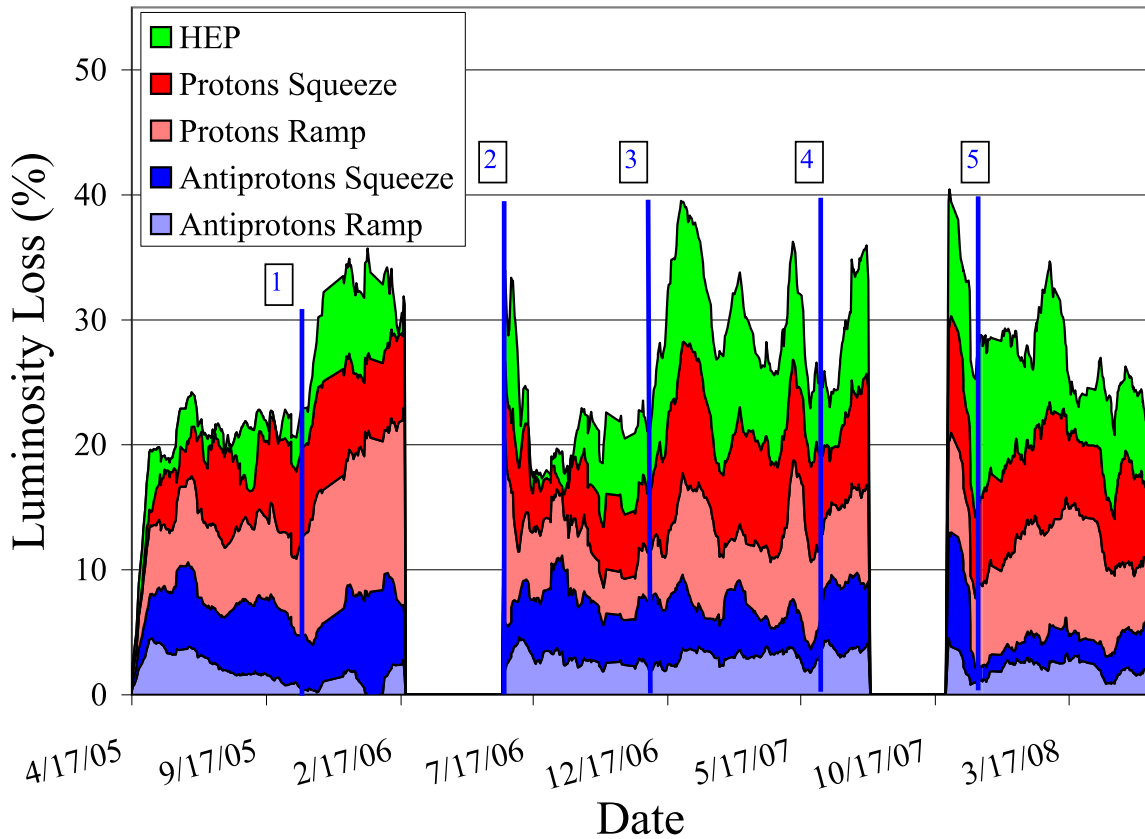


**Figure 2.** Luminosity loss budget over a 3 year period. The labels mark: 1. Commissioning of electron cooling. 2. Installation of extra separators and new collision helix. 3. Antiproton accumulation rate. 4. Correction of second-order chromaticity. 5. Implementation of antiproton emittance blowup.

shape and polarity from injection to collision configuration. The latter posed a serious limitation since the beams separation at several long range collision points briefly decreased from  $5-6\sigma$  to  $\sim 2\sigma$ . At this moment a sharp spike in losses was observed.

Another important operational concern was the tight aperture limitation in one of the two final focus regions (CDF). With dynamically changing orbit and lattice parameters the local losses were often high enough to cause a quench of the superconducting magnets even though the total amount of beam loss was small ( $\sim 1\%$ ). The aperture restriction has been located and fixed in October of 2008.

Besides orbit stability two other factors were found to be important in maintaining low losses through the squeeze: antiproton beam brightness and betatron coupling. Figure 4 shows the dependence of proton losses on the antiproton beam brightness. Large amount of stores lost in this stage of the cycle caused by increase of the antiproton beam brightness after the 2007 shutdown demanded the commissioning of the antiproton emittance control system [9].

### 2.3 High energy physics

After the beams were brought into collisions at the main IPs, there were two head-on and 70 long range collision points per bunch. Beam-beam effects caused by these interactions lead to emittance

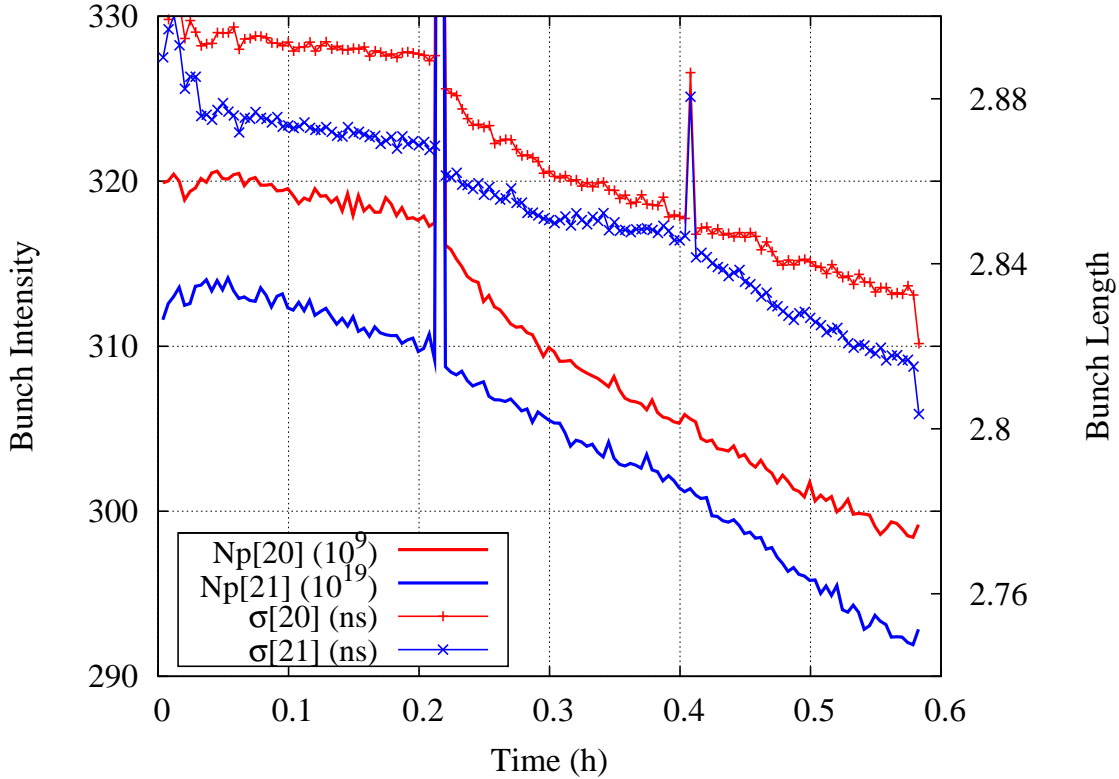


**Figure 3.** Intensity and length of proton bunches no. 20 and 21 during injection of antiprotons.

growth and particle losses in both beams.

During the running prior to the 2006 shutdown the beam-beam effects at HEP mostly affected antiprotons. The long range collision points nearest to the main IPs were determined to be the leading cause for poor life time. Additional electrostatic separators were installed in order to increase the separation at these IPs from  $5.4$  to  $6\sigma$  [8]. Also, the betatron tune chromaticity was decreased from 20 to 10 units. Since then, the antiproton life time was dominated by losses due to luminosity and no emittance growth was observed provided that the betatron tune working point was well controlled.

Electron cooling of antiprotons in the Recycler and increased antiproton stacking rate drastically changed the situation for protons. Figure 5 shows the evolution of total head-on beam-beam tune shift  $\xi$  for protons and antiprotons. Note that prior to the 2006 shutdown the proton  $\xi$  was well under 0.01 and big boost occurred in 2007 when both beam-beam parameters became essentially equal. It was then when beam-beam related losses and emittance blowup started to be observed in protons.

Our analysis showed that deterioration of the proton life time was caused by a decrease of the dynamical aperture for off-momentum particles due to head-on collisions (see Sec. 5.5). It was discovered that the Tevatron optics had large chromatic perturbations, e.g. the value of  $\beta^*$  for off-momentum particles could differ from that of the reference particle by as much as 20%. Also, the high value of second order betatron tune chromaticity  $d^2Q/d\delta^2$  generated a tune spread

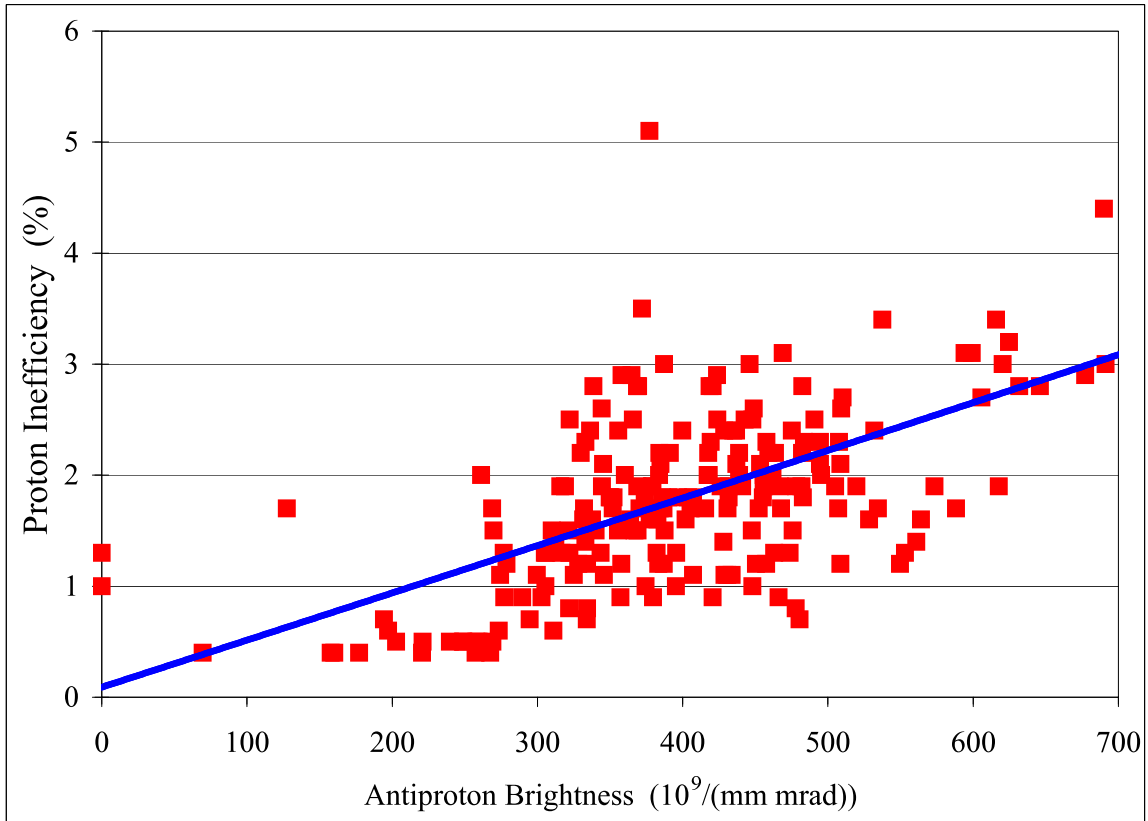


**Figure 4.** Proton losses in low-beta squeeze vs. antiproton beam brightness  $36 \cdot N_a / \epsilon_a$ .

of  $\sim 0.002$ . A rearrangement of sextupoles in order to correct the second order chromaticity was planned and implemented before the 2007 shutdown [10]. Figure 6 demonstrates the effect of this modification on integrated luminosity. Since the dependence of luminosity on time is very well fitted by a  $L_0 / (1 + t/\tau)$  function, one can normalize the luminosity integral for a given store to a fixed length  $T_0$  by using the expression  $L_0 \tau \cdot \ln(1 + T_0/\tau)$  [11]. Here  $L_0$  is the initial luminosity, and  $\tau$  is the luminosity life time. One can see that after the modification the saturation at luminosities above  $2.6 \times 10^{32}$  was mitigated and the average luminosity delivered to experiments increased by  $\sim 10\%$ .

Another step in the proton  $\xi$  happened after the 2007 shutdown when the transverse antiproton emittance decreased because of improvements in injection matching. The total attained head-on beam-beam tune shift for protons exceeded that of antiprotons and reached 0.028. This led to high sensitivity of the proton life time to small variations of the betatron tunes, and to severe background conditions for the experiments. The reason was believed to be the large betatron tune spread generated by collisions of largely different size bunches [12]. Indeed, at times the antiproton emittance was a factor of 5 to 6 smaller than the proton emittance.

To decrease the proton to antiproton emittance ratio a system has been commissioned which increases the antiproton emittance after the top energy is reached by applying wide band noise to a directional strip line (line 5 in Fig. 2) [9]. Ultimately, the optimal emittance ratio was determined to be about  $\sim 3$ .

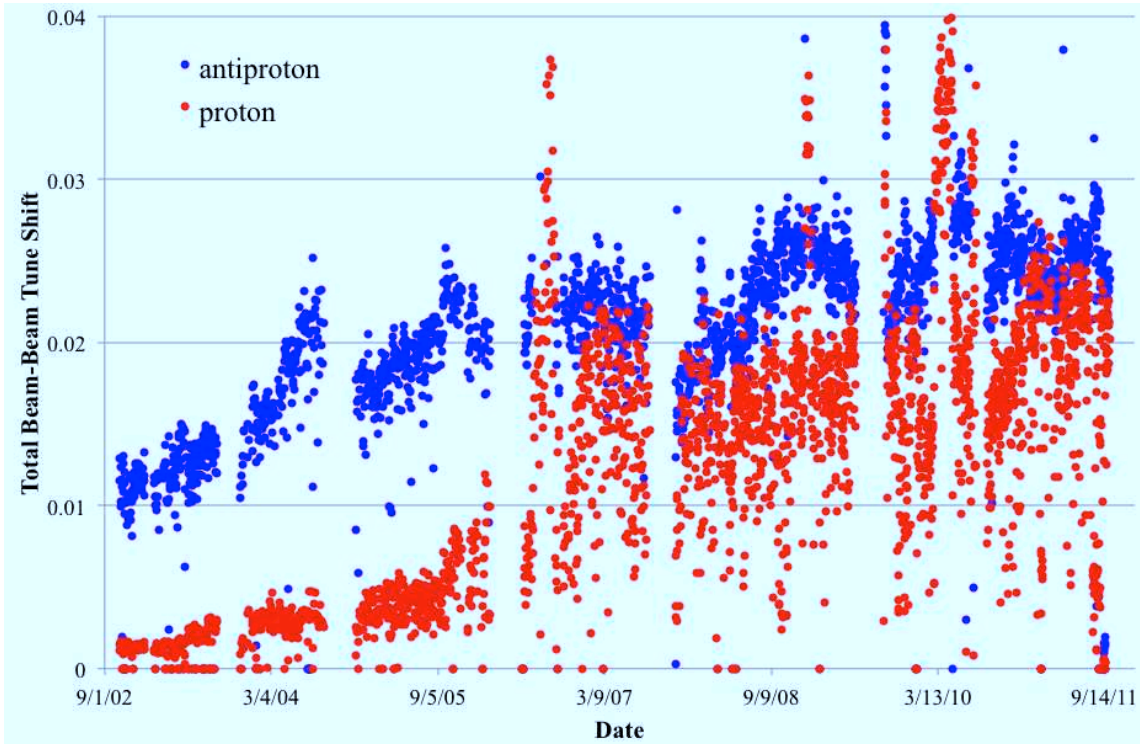


**Figure 5.** Head-on beam-beam tune shift vs. time.

Since the majority of our efforts was targeting beam-beam effects in HEP mode, we concentrate on this topic in the remaining part of this paper. Discussion of long range effects at injection and coherent effects [13] is left out of the scope of this report.

### 3. Store beam physics analysis

Beam-beam interaction was not the single strongest effect determining evolution of beam parameters at collisions. There were many sources of diffusion causing emittance growth and particle losses, including but not limited to intrabeam scattering, noise of accelerating RF voltage, and scattering on residual gas. Parameters of these mechanisms were measured in beam studies, and then a model was built in which the equations of diffusion and other processes were solved numerically [14]. This model was able to predict evolution of the beam parameters in the case of weak beam-beam effects. When these effects were not small, it provided a reference for evaluation of their strength. We used this approach on a store-by-store basis to monitor the machine performance in real time [15] because such calculations were very fast compared to a full numerical beam-beam simulation. Fig. 7 presents an example comparison of evolution of beam parameters in an actual high luminosity store to calculations. Note that there is no transverse emittance blow up in both beams, and the emittance growth is determined by processes other than beam-beam interaction. The same is true for antiproton intensity and bunch length. The most pronounced difference between the observation and the model is seen in the proton intensity. Beam-beam effects caused proton life time degradation during the initial 2-3 hours of the store until the proton beam-beam tune shift drops from 0.02 to 0.015. The corresponding loss of luminosity integral was about 5%.

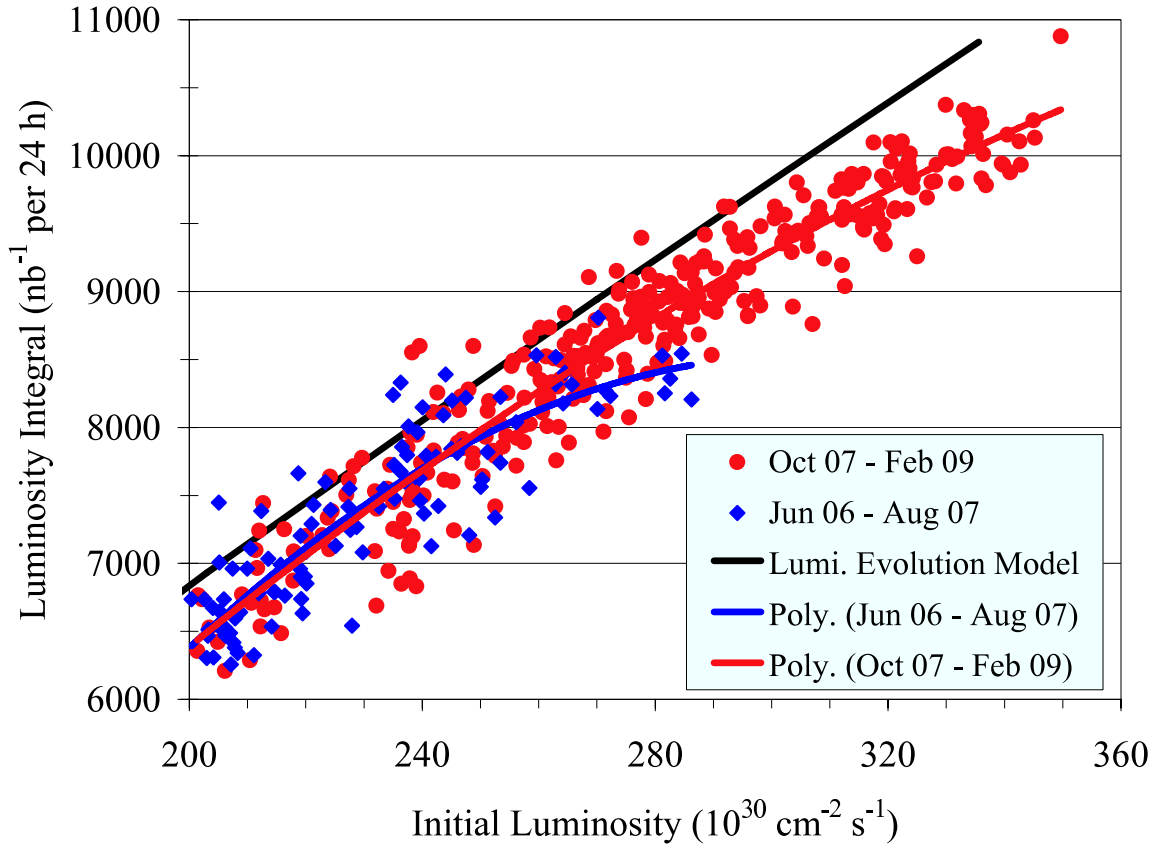


**Figure 6.** Luminosity integral normalized by 24 h vs. initial luminosity. Blue points and curve - before second order chromaticity correction, red - after correction. Black line represents the ultimate integral for the given beam parameters in the absence of beam-beam effects.

#### 4. Weak-strong code Lifetrac

Initially, the beam-beam code LIFETRAC was developed for simulation of the equilibrium distribution of the particles in circular electron-positron colliders [16]. In 1999 the new features have been implemented, which allowed simulating non-equilibrium distributions, for example proton beams. In this case the goal of simulations is not to obtain the equilibrium distribution but to observe how the initial distribution is changing with time. Number of simulated particles can vary in the range of  $10^3$  to  $10^6$ , usually it is set to  $(5 \div 10) \cdot 10^3$ . The tracking time is divided into “steps”, typically  $10^3 \div 10^5$  turns each. The statistics obtained during the tracking (1D histograms, 2D density in the space of normalized betatron amplitudes, luminosity, beam sizes and emittances) is averaged over all particles and all turns for each step. Thus, a sequence of frames representing evolution of the initial distribution is obtained.

Another important quantity characterizing the beam dynamics is the intensity life time. It is calculated by placing an aperture restriction in the machine and counting particles reaching the limit. The initial and final coordinates of the lost particle are saved. This information is valuable for analysis of various beam dynamics features.

The initial 6D distribution of macroparticles can be either Gaussian (by default), or read from

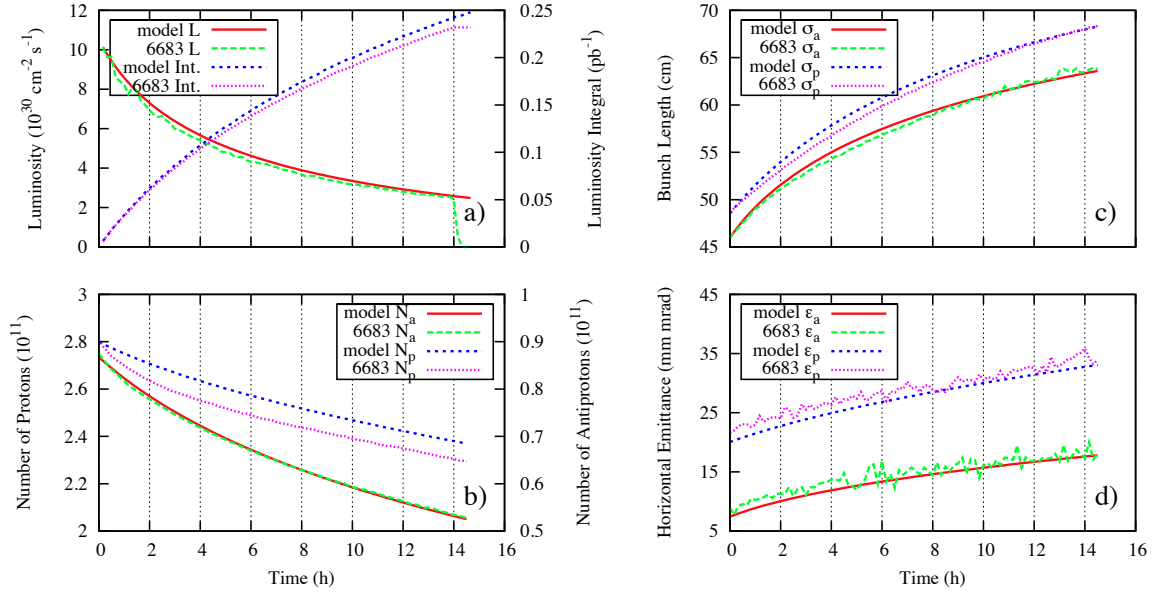


**Figure 7.** Observed beam parameters in store 6683 compared to store analysis calculation (model).  $L_0 = 3.5 \cdot 10^{32} \text{cm}^{-2} \text{s}^{-1}$ . a) Single bunch Luminosity and Luminosity integral. b) Intensity of proton bunch no. 6 and of antiproton bunch colliding with it (no. 13). c) Bunch lengths. d) Horizontal 95% normalized bunch emittances.

a separate text file. Besides, the macroparticles may have different “weights”. This allows representing the beam tails more reliably with limited number of particles. Usually we simulate the Gaussian distribution with weights: particles initially located in the core region have larger weight while the “tail” particles with smaller weight are more numerous.

In the Tevatron bunch pattern (3 trains of 12 bunches) there are two main IPs and 70 long range collision points for each bunch. When performing transformation through a main IP, the “strong” bunch is divided into slices longitudinally. The higher are the orders of significant betatron resonances which are supposed to make effect on the distribution, the greater must be the number of slices. In our simulations 12 slices were used in the main IPs where beta-functions are approximately equal to the bunch length and only one slice in long range collision points where beta-functions are much greater and one can neglect the betatron phase advance on the bunch length.

The transverse density distributions within “strong” slices are bi-Gaussian, allowing to apply the well-known formulae [17] for 6D symplectic beam-beam kick. However, a simple modification allowed simulating non-Gaussian strong bunches. Namely, the strong bunch is represented as a superposition of a few (up to three) Gaussian distributions with different betatron emittances. The kicks from all these “harmonics” are summarized additively. The calculation time is increased somehow (not very significantly) but the transformation remains 6D symplectic.

#### 4.1 Tevatron optics

The parasitic collisions in Tevatron played a significant role in the beam dynamics. In order to for account their contribution correctly an accurate knowledge of the machine lattice of the whole ring

with all distortions, beta beatings, coupling, etc. was required. This necessitated the construction of a realistic model of the machine lattice based on beam measurements. The most effective method proved to be the orbit response matrix analysis [18, 19, 20].

The model lattice was built in the optics code OptiM [21]. Both OptiM and Lifetrac treat betatron coupling using the same coupled beta-functions formalism [22]. This allows the linear transport matrix between any two points to be easily derived from the coupled lattice functions and phase advances.

A set of scripts has been created enabling fast creation of input files for the beam-beam simulation. These programs automate calculation of azimuthal positions of interaction points for the chosen bunch and extraction of the optics parameters. In the end, the machine optics is represented by a set of 6D linear maps between the interaction points.

It was estimated that resonances generated by known Tevatron nonlinearities, such as the final focus triplets and lattice sextupoles, were much weaker than those driven by beam-beam collisions at the operational betatron tune working point. Hence, inclusion of nonlinear lattice elements into the simulation was deemed unnecessary. Still, the code has the capability to include thin multipoles up to 10-th order.

## 4.2 Chromaticity

Although linear optics is used for the machine lattice model, there are two nonlinear lattice effects which are considered to be significant for beam-beam behaviour and were included into simulations. These are the chromaticities of beta-functions excited in the main IPs and chromaticities of the betatron tunes. In the Hamiltonian theory the chromaticity of beta-functions does not come from energy-dependent focusing strength of quads (as one would intuitively expect) but from drift spaces where the transverse momentum is large (low-beta regions). The symplectic transformations for that are:

$$\begin{aligned} X &= X - L \cdot X' \cdot \frac{\Delta p}{p} \\ Y &= Y - L \cdot Y' \cdot \frac{\Delta p}{p} \\ Z &= Z - L \cdot (X'^2 + Y'^2)/2 \end{aligned}$$

where  $X$ ,  $Y$ , and  $Z$  are the particle coordinates, and  $L$  is the ‘‘chromatic drift’’ length. Then, it is necessary to adjust the betatron tune chromaticities which are also affected by ‘‘chromatic drift’’. For that, an artificial element (insertion) is used with the following Hamiltonian:

$$H = I_x \cdot (2\pi Q_x + C_x \frac{\Delta p}{p}) + I_y \cdot (2\pi Q_y + C_y \frac{\Delta p}{p}),$$

where  $I_x$  and  $I_y$  are the action variables,  $Q_x$  and  $Q_y$  are the betatron tunes,  $C_x$  and  $C_y$  are the [additions to the] chromaticities of betatron tunes.

## 4.3 Diffusion and noise

Diffusion and noise are simulated by a single random kick applied to the macroparticles once per turn. Strength of the kick at different coordinates is given by a symmetrical matrix representing

correlations between Gaussian noises. In the Tevatron, the diffusion was rather slow in terms of the computer simulation – the characteristic time for the emittance change was around an hour, or  $\sim 10^8$  turns. In simulations aimed at evaluation of the antiproton beam dynamics during the 2004-2005 run the noise was artificially increased by three orders of magnitude in order to match the diffusion and the computer capabilities.

We justify this approach below. In contrast to the electron-positron colliders there is no damping in hadron colliders. As the result, during the store time an effect of beam-beam interaction on the emittance growth needs to be minimized and made small relative to other diffusion mechanisms such as the intra-beam scattering (IBS), scattering on the residual gas, and diffusion due to RF phase noise. We will call these the extrinsic diffusion to distinguish from the diffusion excited by beam-beam effects. For the 2005 Tevatron parameters the extrinsic diffusion set the luminosity lifetime to be about 10 hours at the beginning of the store. IBS dominated both transverse and longitudinal diffusions in the case of protons while its relative effect was significantly smaller for antiprotons because of  $\sim 5$  times smaller intensity.

Table 1 summarizes lifetimes for major beam parameters obtained with diffusion model [23] for a typical 2005 Tevatron store with the luminosity of  $0.9 \times 10^{32} \text{cm}^{-2} \text{s}^{-1}$ . There were many parameters in Tevatron which are beyond our control and therefore each store was different. For good stores, the beam-beam effects made comparatively small contribution to the emittance growth yielding luminosity lifetime in the range of 7-8 hours and 10-15% loss in the luminosity integral.

<b>Parameter</b> (lifetime, hour)	<b>Protons</b>	<b>Antiprotons</b>
Luminosity	9.6	9.6
Transverse emittance, $(d\varepsilon/dt)/\varepsilon$ [hor./vert.]	-17 / -18	-52 / -46
Longitudinal emittance	-8	-26
Intensity	26	155

**Table 1.** Lifetimes for major beam parameters obtained with diffusion model.

Under the real conditions at Tevatron the emittance growth rate was small and exact simulations of beam-beam effects would require tracking for billions of turns. That is well beyond capabilities of present computers. Fortunately, the extrinsic diffusion is large enough in comparison with beam-beam diffusion, which results in the loss of phase correlation after about 50,000 turns.

The external noise plays important role in particle dynamics: it provides particle transport in the regions of phase space which are free from resonance islands.

To make this transport faster we can artificially increase the noise level assuming that its effect scales as noise power multiplied by number of turns. If we choose it so that the noise alone gives 10% emittance growth in  $10^6$  turns (we use this level as the reference) then this number of turns of simulation will correspond to  $\sim 5$  h of time in the Tevatron.

To verify this approach we studied the effect of the noise level on luminosity using the reconstructed optics.

Fig. 8 presents the results of tune scan along the main diagonal with the reference noise level and without noise. The effect of noise on luminosity corresponds to its level with exception for the point  $Q_y = 0.575$  where it was larger due to some cooperation with strong 5th order resonances.

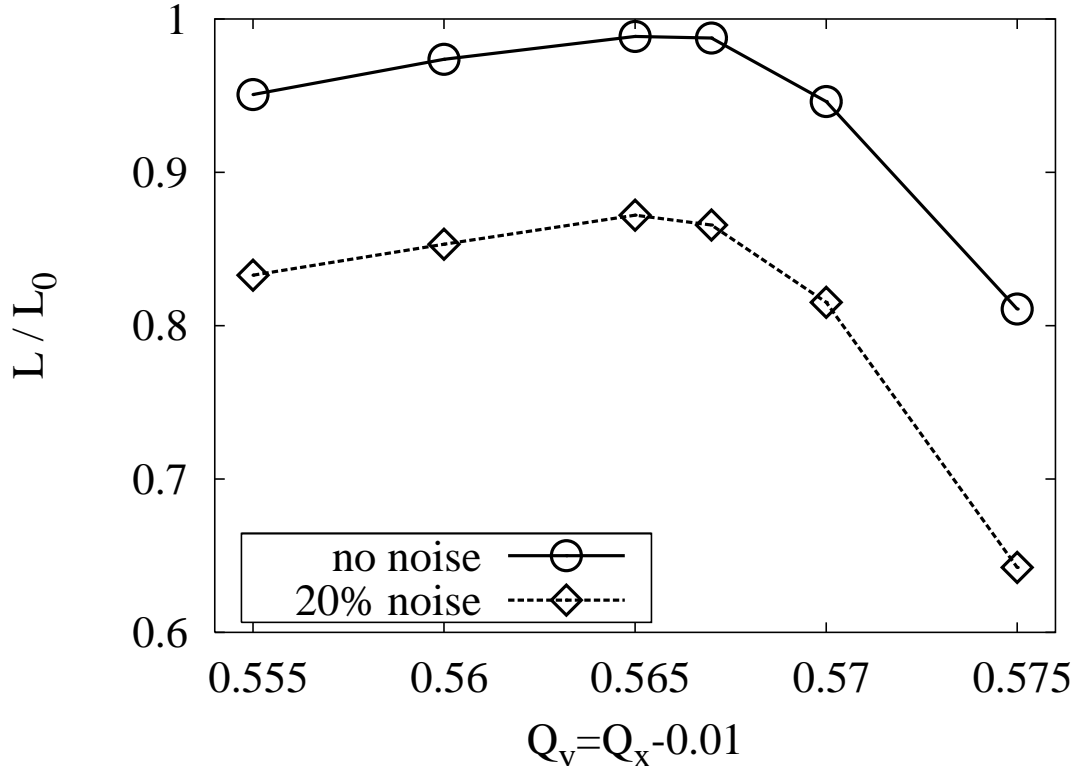


**Figure 8.** Ratio of luminosity after a fixed time ( $t = 2 \cdot 10^6$  turns) to the initial luminosity vs. betatron tune. Circles -  $D_{noise} = 0$ , diamonds - the emittance change due to extrinsic diffusion after  $t$  is 20%.

To study this cooperation in more detail we performed tracking at this working point with different noise levels. Fig.9 shows the luminosity reduction in  $2 \cdot 10^6$  turns (diamonds) and a fit made using just 3 points, with relative noise level 0.5, 1 and 2.

The fit works fine for higher noise level, but predicts somewhat faster luminosity decay in the absence of noise than actually observed in tracking. This means that there are regions in the phase space which particles cannot pass (within the tracking time) without assistance from the external noise so that the simple rule  $D_{total} = D_{res} + D_{noise}$  does not apply. However, such “blank spaces” may contain isolated resonance islands which would show up on a longer time scale with the real level of external noise. The applicability of this rule at the reference noise level testifies that (with the chosen number of turns) no such “blank spaces” were left so we get more reliable predictions.

Since 2007 we do no longer use the artificial noise enhancement for two reasons: a) the time interval of interest became shorter (less than one hour) after the shift of focus in beam-beam effects from antiprotons to protons; b) over the years the available computing power was constantly increasing and a simulation of  $10^7$  turns (corresponding to 210 s of real time) takes about 20 hours on a modern computing cluster.

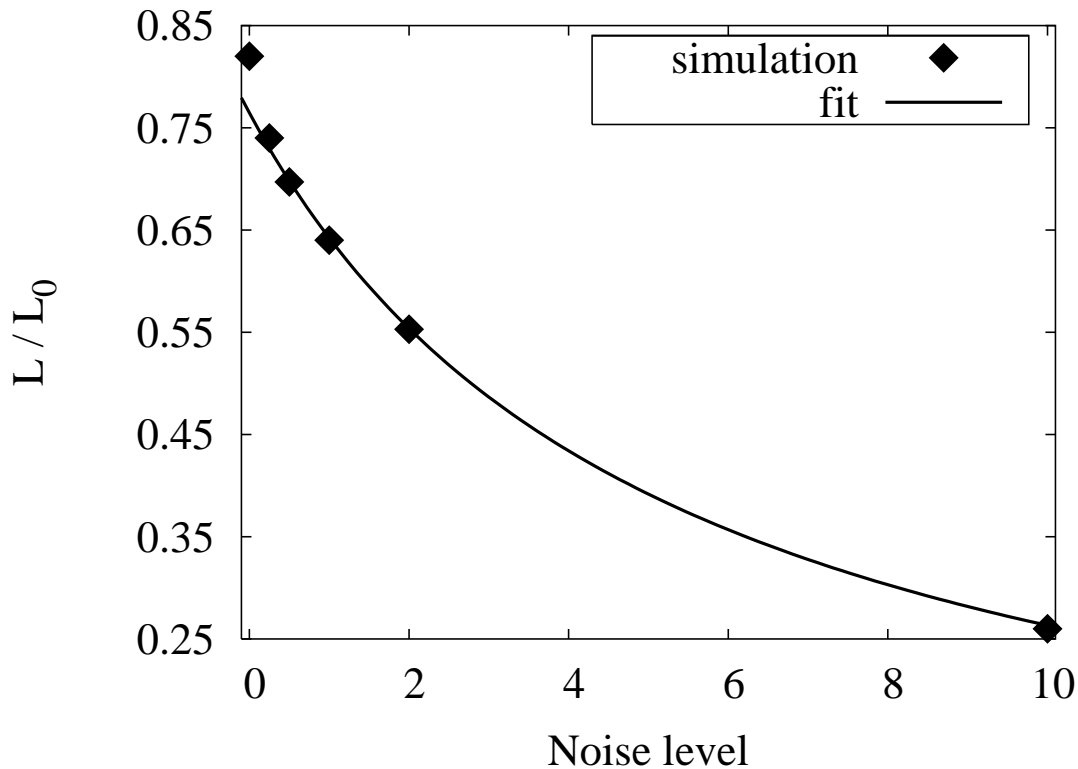


**Figure 9.** Ratio of luminosities vs. noise level.

#### 4.4 Program features

Since the beam-beam code uses the “weak-strong” model, it can be very efficiently parallelized. Each processor tracks its own set of particles and the nodes need to communicate very rarely (at the end of each step), just to gather the obtained statistics. Hence, the productivity grows almost linearly with the number of nodes.

There are also two auxiliary GUI codes. The first one automates production of the Linetrac input files for different bunches from the OptiM machine lattice files. The second one is dedicated for browsing the Lifetrac output files and presenting the simulation results in a text and graphical (histogram) form.

#### 4.5 Code validation

We have validated the code using available experimental data. As an example, Figs. 10 and 11 show a good reproduction of the two distinct effects in bunch to bunch differences caused by beam-beam effects: variation of vertical bunch centroid position due to long range dipole kicks, and variation of transverse emittance blowup caused by difference in tunes and chromaticities. We also demonstrated that scallops can be reduced by moving the working point farther from 5th order resonance.

In addition, the code was validated against another weak-strong tracking tool Sixtrack on the case of the Large Hadron Collider, and good agreement was observed [24]

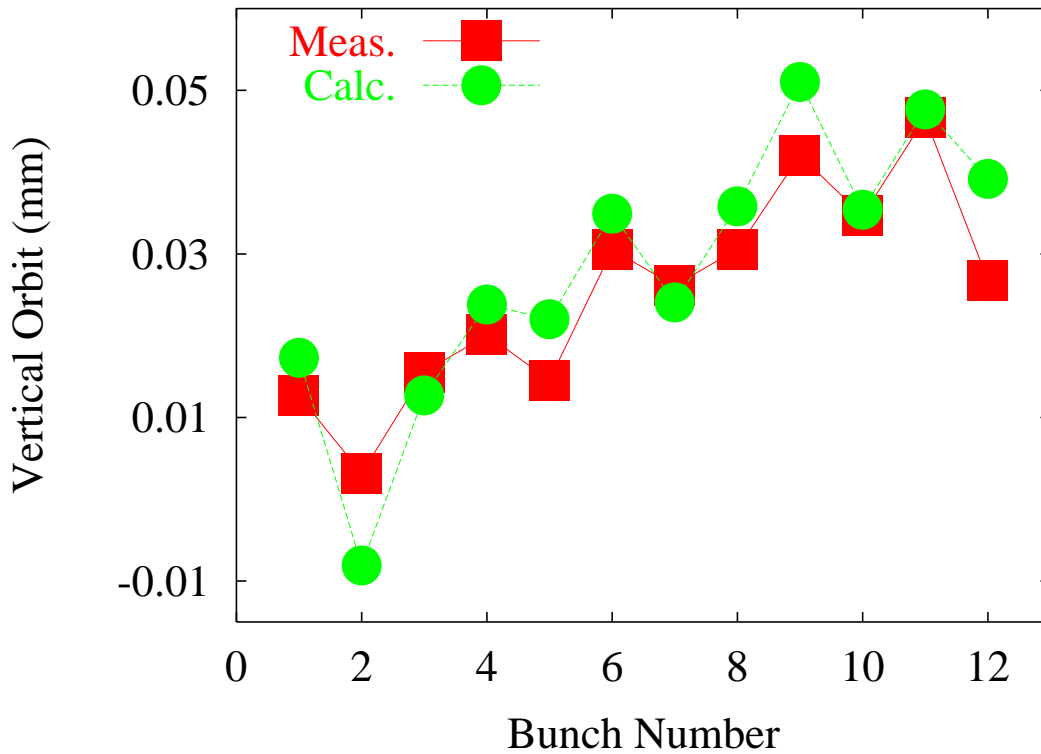


**Figure 10.** Bunch by bunch antiproton vertical orbit.

## 5. Simulation results

Simulations with Lifetrac played an important role in justification of many collider configuration changes, which resulted in performance improvements. These changes include the decrease of antiproton betatron tune chromaticity, reduction of the  $\beta^*$  from 0.35 m to 0.28 m (both in 2005), correction of the collision optics, increase of separation at the long range collision points nearest to the main IPs, and correction of the chromatic beta-function. In this section we present the selected simulation results for some of these topics.

### 5.1 Optics errors

Early in the Run II it was recognized that the Tevatron collision optics had significant distortions caused by the systematic betatron coupling resulting from the coil creep in main dipoles [25], imperfect machine modeling and other sources. We measured the machine optics using LOCO method and performed simulations with Lifetrac for different optics versions. In the results presented below we used 3 major optics modifications:

- “design” optics with ideal parameters of the main IPs, zero coupling.
- “january” optics which was in effect until March, 2004. This optics was measured in January, 2004, and had sufficient distortions in the main IPs (unequal beta’s, beam waists shifted from the IP), and betatron coupling.

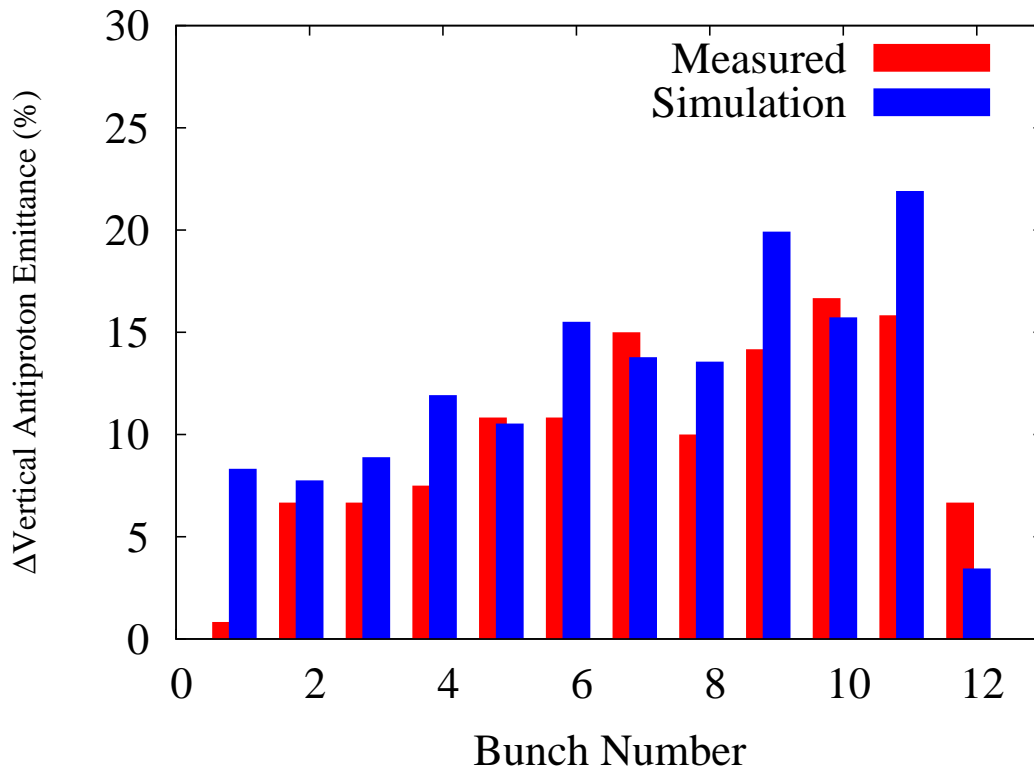


**Figure 11.** Bunch by bunch antiproton emittance growth. Measured in store 3554 (red) and simulated with lifetrac (blue).

- “june” optics introduced in March, 2004, where the distortions were corrected.

Comparison of the three cases is shown in Fig. 12. This plot shows that modifications to the optics implemented in March, 2004, made the optics close to the design. Additional simulations revealed that the main source of particle losses was in the long range collisions (PC) nearest to the main IPs. Increasing the beams separation in these points and repairing the phase advances cured high antiproton losses.

## 5.2 New collision helix

As mentioned, the strong betatron resonances affecting the collider performance were caused by beam-beam effects. It was shown analytically that the strength of the 7-th order resonance was determined by the long range collisions [8]. Our simulations predicted that increasing the beam separation at the Parasitic Collision (PC) points nearest to the main IPs would give the largest benefit. The significance of the PCs is illustrated in Fig. 13, where a bunch intensity is plotted vs. time ( $2 \times 10^6$  turns in this simulation correspond to about 15 hours in the Tevatron) with the complete set of IPs and PCs, and with the most significant PCs turned off. It is clear that PCs dominate the particle losses.

To increase separation at these PCs, two extra electrostatic separators were installed during the 2006 shutdown. As the result of their commissioning, the separation at the IPs upstream and

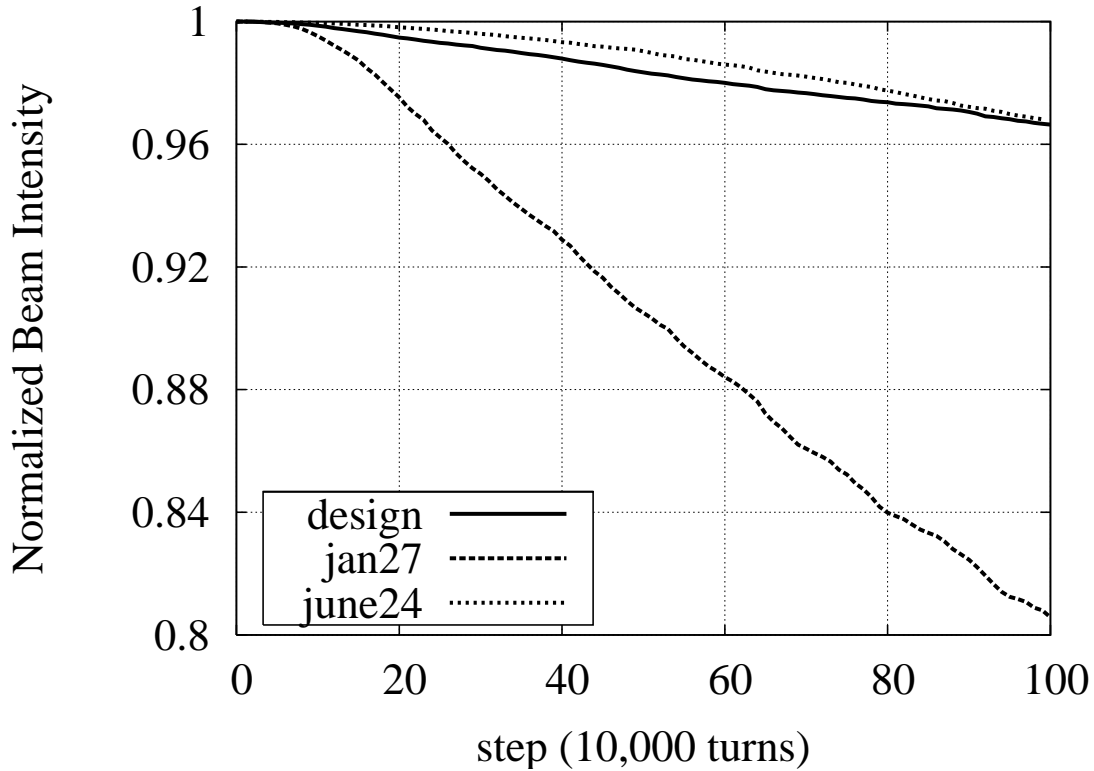


**Figure 12.** Intensity of antiproton bunch #6 vs. time for different types of optics.  $\xi = 0.01$ ,  $Q_x = 0.57$ ,  $Q_y = 0.56$

downstream of CDF and D0 increased by 20% (Table 2). The increased separation showed itself in improved beam lifetime and allowed to push the intensity limit further.

	CDF u.s.	CDF d.s.	D0 u.s.	D0 d.s.
<b>Before</b>	5.4	5.6	5.0	5.2
<b>After</b>	6.4	5.8	6.2	5.6

**Table 2.** Radial separations in the first long range collision points in units of the beam size.

Figure 14 shows a comparison of the single bunch luminosity and luminosity integral for two HEP stores before and after commissioning of the new helix. Initial intensities and emittances of antiprotons in these stores were close which allows direct comparison. As one can see, luminosity lifetime in the new configuration has improved substantially. The overall gain can be quantified in terms of luminosity integral over a fixed period of time (e.g. 24 hours) normalized by the initial luminosity. The value of this parameter has increased by 16%.

### 5.3 Chromaticity

Reducing the betatron tune chromaticity can also be a very powerful instrument in decreasing the particle losses. Simulation results in Fig. 15, demonstrate that changing the tune chromaticity

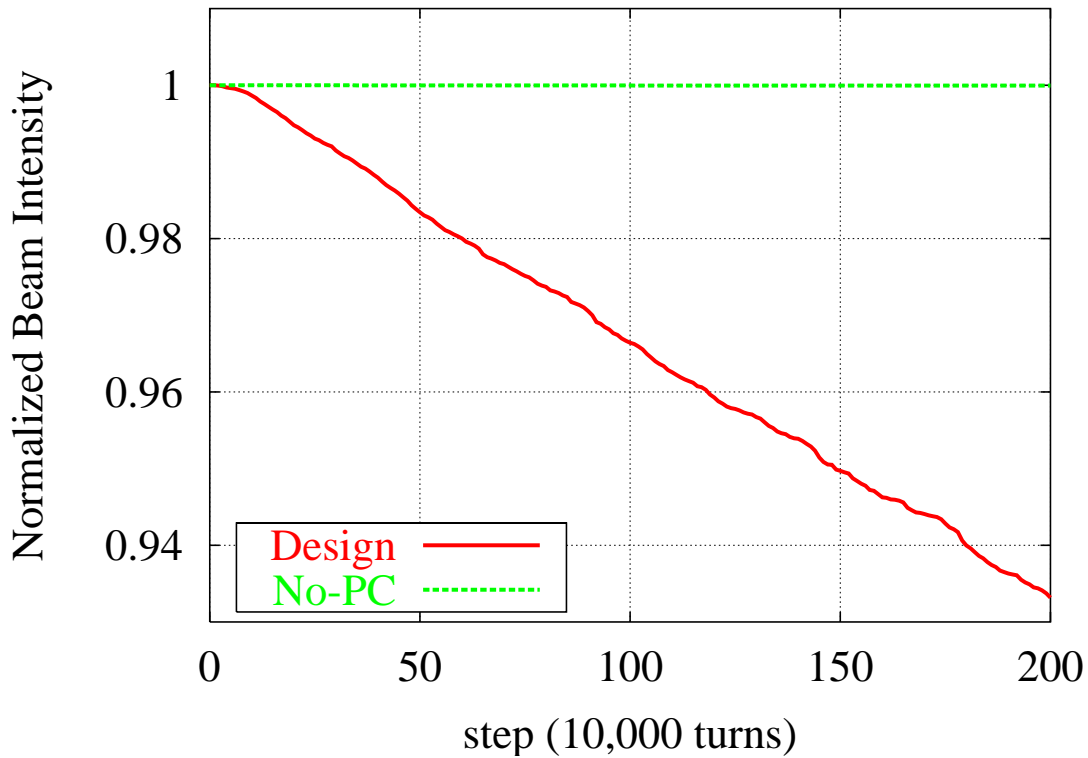


**Figure 13.** Normalized intensity of bunch #6 simulated in the presence (solid line) and in the absence (dashed line) of long range collisions.

from 15-20 units to 5-10 units may significantly improve the beam life time. This change was implemented in 2006 and resulted in about 10% gain in luminosity integration rate. The safe lower limit of the tune chromaticity was determined by the coherent stability of the beams. It was demonstrated experimentally that with head-on collisions initiated, the beams remained stable even at zero chromaticity. Apparently, the Landau damping by strong nonlinearity of the head-on beam-beam was the major factor. However, in the routine operation the typical value of chromaticity was approximately 5.

#### 5.4 $\beta^*$ reduction

An improvement which could be relatively easily implemented was the reduction of the beta-function at the main IPs. Decreasing the  $\beta^*$  from the design value of 0.35 m to 0.28 m resulted in 10% both in peak luminosity and in luminosity integral. However, further improvement along this route was not practical due to the hourglass effect and rather significant increase of the maximum beta-function in the final focus triplet, and subsequent engagement of effects related to the magnet vibrations and aperture limitation.

#### 5.5 Second order chromaticity

Increasing the beam separation mitigated the long range beam-beam effects. However, with advances in the antiproton production rate, the initial antiproton intensity at collisions has been rising

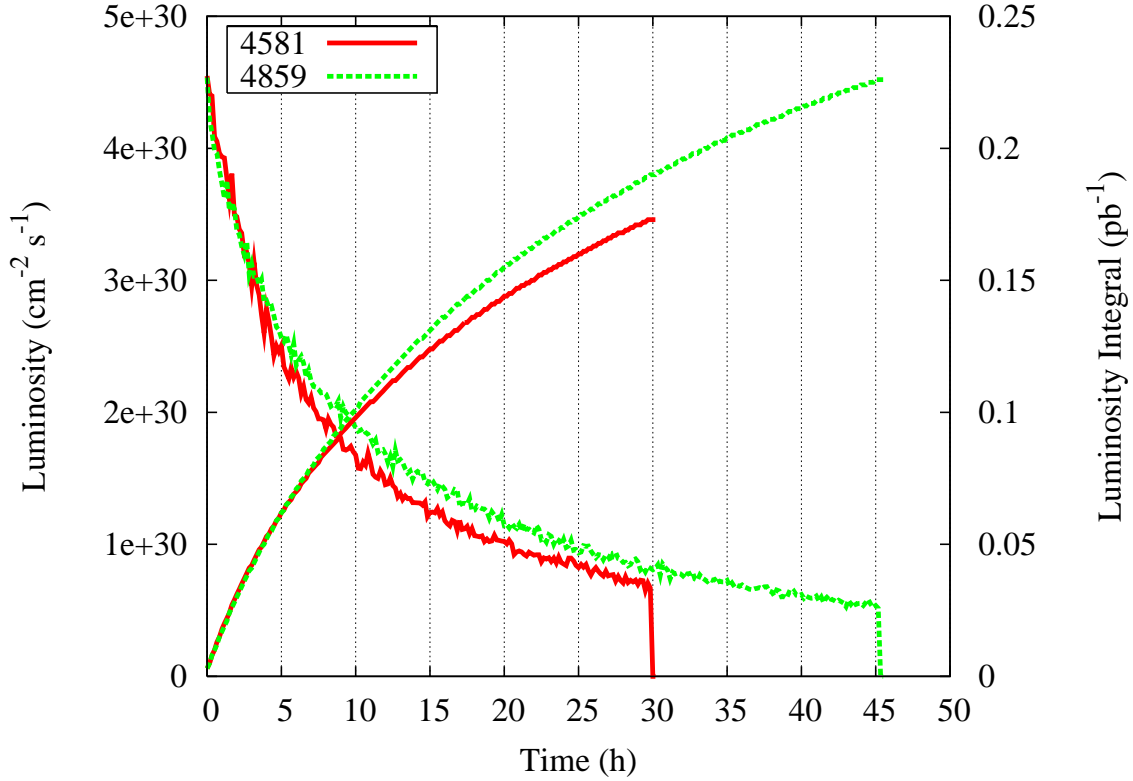


**Figure 14.** Single bunch luminosity and luminosity integral for stores 4581 and 4859.

continuously. In 2006, the head-on beam-beam parameter for protons was pushed up to 0.008 per IP which made the head-on beam-beam effects in the proton beam much more pronounced. One of the possible ways for improvement was a major change of the betatron tune in order to increase the available tune space. This, however, required significant investment of the machine time for optics studies and tuning. A partial solution could be implemented by decoupling of the transverse and longitudinal motion at the main IPs, i.e. by reducing the chromatic beta-function.

The value of chromatic beta-function  $(\Delta\beta/\beta)/(\Delta p/p)$  at both IPs in the original Tevatron lattice was -600 which lead to the beta-function change of 10% for a particle with  $1\sigma$  momentum deviation [10]. Thus, a large variation of focusing for particles in the bunch existed giving rise to beam-beam driven synchrotron resonances.

Planning for the increase in amount of antiprotons available to the collider, we identified the large chromaticity of  $\beta^*$  as a possible source of the proton life time deterioration. Figure 16 shows the beam-beam induced proton life time for different values of  $\xi$ , and demonstrates the positive effect of corrected chromatic  $\beta^*$ .

Simulations revealed an interesting feature in the behavior of the proton bunch length at high values of  $\xi$  - the so-called bunch shaving, when the bunch length starts to decrease after initiating head-on collisions instead of steady growth predicted by the diffusion model (Fig. 17). This behavior was observed multiple times during HEP stores in 2007, being especially pronounced when the vertical proton betatron tune was set too high.

In order to achieve the desired smaller beta-function chromaticity, a new scheme of sextupole

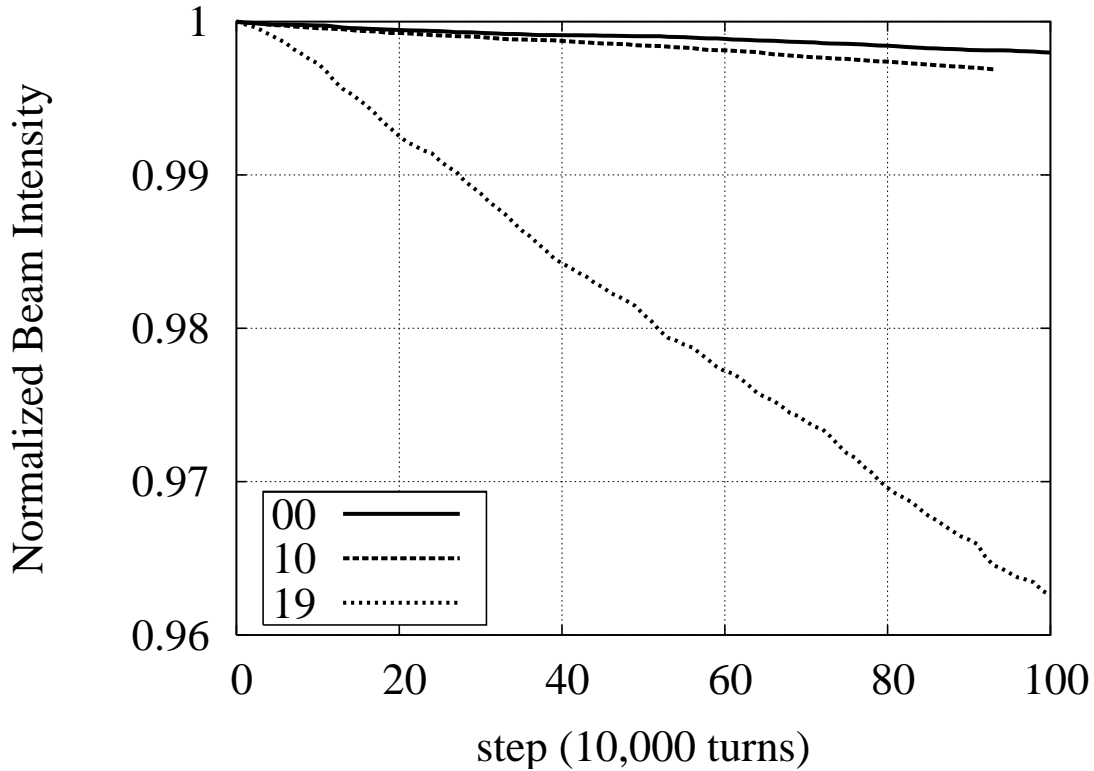


**Figure 15.** Evolution of the antiproton bunch intensity for various values of betatron tune chromaticity.  $Q_x = 0.58$ ,  $Q_y = 0.575$ ,  $\xi = 0.01$ .

correctors in the Tevatron has been developed and implemented in May of 2007. The scheme used the existing sextupole magnets split into multiple families instead of just two original SF and SD circuits. The effect of introducing the new circuits is illustrated in Fig. 6.

## 6. Summary and discussion

Over the last four years of Run II Tevatron routinely operated at the values of head-on beam-beam tune shift for both proton and antiproton beams exceeding 0.02. The transverse emittance of antiprotons was a factor of 3 to 5 smaller than the proton emittance. This created significantly different conditions for the two beams.

Beam-beam effects in antiprotons were dominated by long range interactions at four collision points with minimal separation. After the separation at these points was increased to  $6\sigma$  no adverse effects were observed in antiprotons at present proton intensities.

On the contrary, protons experienced life time degradation due to head-on collisions with the beam of smaller transverse size. Correction of chromatic  $\beta$ -function in the final focus and reduction of betatron tune chromaticity increased dynamic aperture and improved proton beam life time.

Weak-strong simulation of beam-beam effects with Lifetrac code developed for the Tevatron correctly describes many observed features of the beam dynamics, has predictive power and has been used to support changes of the machine configuration.

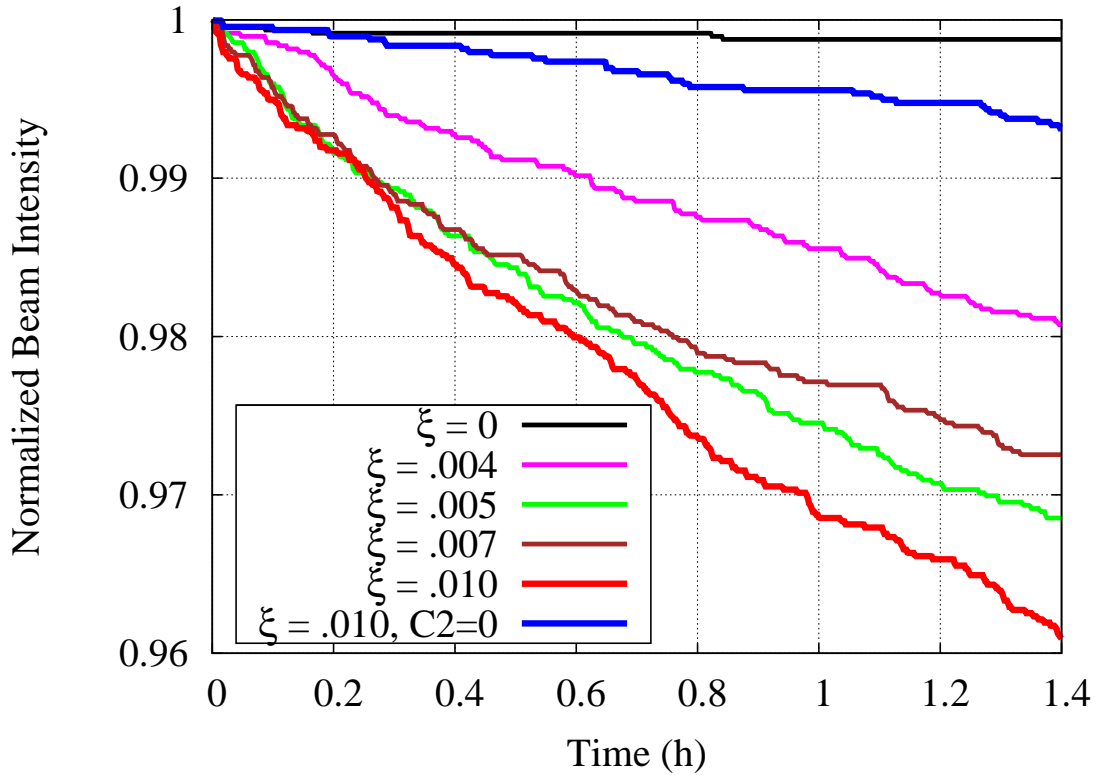


**Figure 16.** Proton intensity evolution for different values of beam-beam parameter per IP.

Further increase of the beam intensities was limited by the space available on the tune diagram near the operational working point. A change of the tune working point from 0.58 to near the half integer resonance would allow as much as 30% increase of intensities but required a lengthy commissioning period which rendered this improvement impossible in Run II.

## Acknowledgments

This work was made possible by hard work and dedication of many people at Fermilab. Fermilab is operated by Fermi Research Alliance, LLC under Contract No. DE-AC02-07CH11359 with the United States Department of Energy.

## References

- [1] S. Holmes, R.S. Moore, and Vladimir Shiltsev, *Overview of the Tevatron collider complex: goals, operations and performance*, 2011 JINST **6** T08001.
- [2] S. Nagaitsev et al., *Experimental demonstration of relativistic electron cooling*, *Phys. Rev. Lett.* **96** (2006) 044801.
- [3] V. Shiltsev et al., *Beam-beam effects in the Tevatron*, *Phys. Rev. ST Accel. Beams* **8** (2005) 101001.
- [4] P.M. Ivanov et al., *Head-tail instability at Tevatron*, in proceedings of *the Particle Accelerator Conference*, 2003, Portland, OR, USA, pp. 3062-3064.

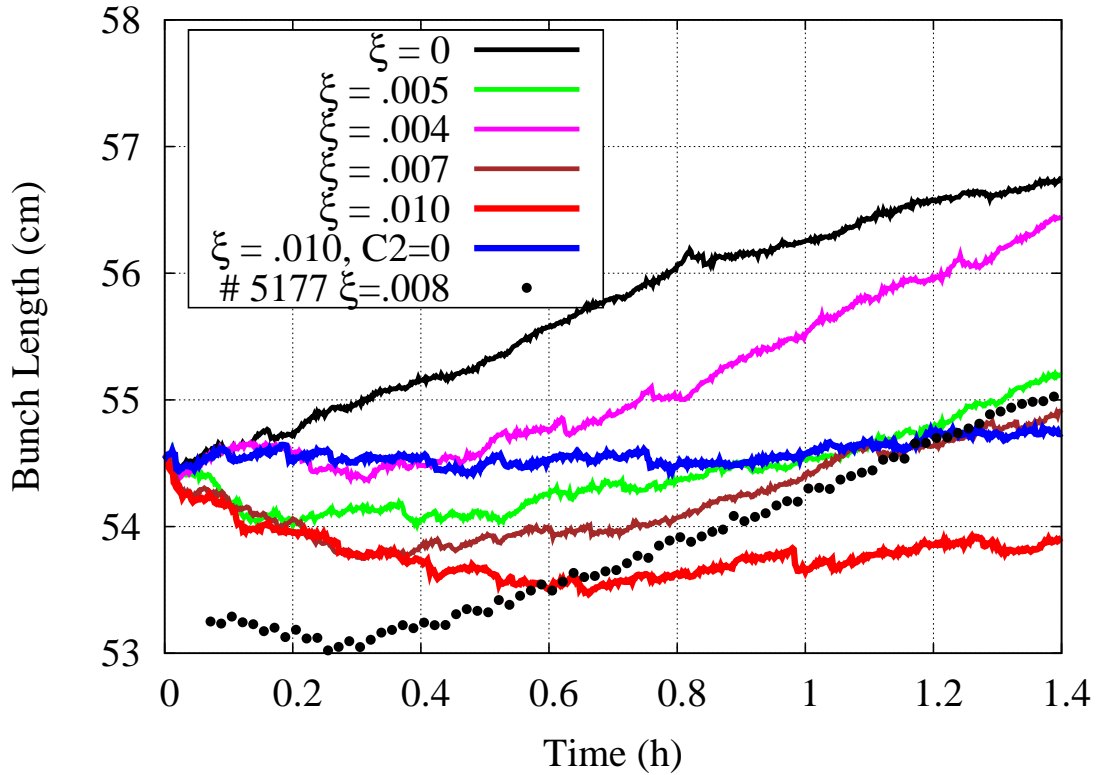


**Figure 17.** Effect of corrected second order chromaticity on the proton bunch length evolution.

- [5] P.M. Ivanov et al., *Landau damping of the weak head-tail instability at Tevatron*, in proceedings of the *Particle Accelerator Conference*, 2005, Knoxville, TN, USA, pp. 2714-2716.
- [6] V.H. Ranjbar and P.M. Ivanov, *Chromaticity and wakefield effect on the transverse motion of longitudinal bunch slices in the Fermilab Tevatron*, *Phys. Rev. ST Accel. Beams* **8** (2008) 084401.
- [7] R.S. Moore et al., *Improving the Tevatron collision helix*, in proceedings of the *Particle Accelerator Conference*, 2005, Knoxville, TN, USA, pp. 1931-1933.
- [8] Y. Alexahin, *Optimization of the helical orbits in the Tevatron*, in proceedings of the *Particle Accelerator Conference*, 2007, Albuquerque, NM, USA, pp. 3874-3876.
- [9] C.Y. Tan and J. Steimel, *Controlled emittance blow up in the Tevatron*, in proceedings of the *Particle Accelerator Conference*, 2009, Vancouver, BC, Canada.
- [10] A. Valishev et al., *Correction of second order chromaticity at Tevatron*, in proceedings of the *Particle Accelerator Conference*, 2007, Albuquerque, NM, USA, pp. 3922-3924.
- [11] V. Shiltsev and E. McCrory, *Characterizing luminosity evolution in the Tevatron*, in proceedings of the *Particle Accelerator Conference*, 2005, Knoxville, TN, USA, pp. 2536-2537.
- [12] M. Syphers, *Beam-beam tune distributions with differing beam sizes*, Fermilab Beams Doc. 3031 (unpublished).
- [13] Yu. Alexahin, *Theory and reality of beam-beam effects at hadron colliders*, in proceedings of the *Particle Accelerator Conference*, 2005, Knoxville, TN, USA, pp. 544-548.

- [14] V. Lebedev, *Beam physics at Tevatron complex*, in proceedings of the *Particle Accelerator Conference*, 2003, Portland, OR, USA, pp. 29-33.
- [15] A. Valishev, *Tevatron store analysis package*,
- [16] D. Shatilov, *Beam-beam simulations at large amplitudes and lifetime determination*, *Part. Accel.* **52** (1996) pp. 65-93.
- [17] K. Hirata, H. Moshhammer and F. Ruggiero, KEK Report 92-117 (1992) (unpublished)
- [18] V. Sajaev et al., *Fully coupled analysis of orbit response matrices at the FNAL Tevatron*, in proceedings of the *Particle Accelerator Conference*, 2005, Knoxville, TN, USA, pp. 3662-3664.
- [19] A. Valishev et al., *Progress with collision optics of the Fermilab Tevatron collider*, in proceedings of the *European Particle Accelerator Conference*, 2006, Edinburgh, Scotland, pp. 2053-2055.
- [20] V. Lebedev et al., *Measurement and correction of linear optics and coupling at tevatron complex*, *Nucl. Instrum. Methods Phys. Res., Sect. A* **558** (2006) p. 299.
- [21] V. Lebedev, *Optim code*,
- [22] V. Lebedev and A. Bogacz, *Betatron motion with coupling of horizontal and vertical degrees of freedom*, 2010 *JINST* **5** P10010.
- [23] V. Lebedev and A. Burov, *Collective instabilities in the Tevatron complex*, in proceedings of the *33rd ICFA advanced beam dynamics workshop on high intensity and high brightness hadron beams*, 2004, Bensheim, Germany, pp. 350-354.
- [24] F. Schmidt, A. Valishev and Y. Luo, *Development and benchmarking of codes for simulation of beam-beam effects at the LHC*, BNL C-A/AP/443 (unpublished).
- [25] G.E. Annala, D.J. Harding and M.J Syphers, *Coil creep and skew-quadrupole field components in the Tevatron*, 2012 *JINST* **7** T03001.